Nucleating Agents for High-Density Polyethylene—A Review

Karl M. Seven,[1] Jeffrey M. Cogen,[1] James F. Gilchrist[2]
[1] *The Dow Chemical Company, Collegeville, Pennsylvania*
[2] *Department of Chemical and Biomolecular Engineering, Lehigh University, Bethlehem, Pennsylvania*

A review of nucleating agent (NA) types and their effect on crystallization in high-density polyethylene (HDPE) is presented. The focus is on methods to improve the physical properties of HDPE due to its widespread use in commercial applications and high volume use in typical industrial processes including extrusion, injection molding, and blow molding. The crystallization process in HDPE significantly affects its final optical, mechanical, and thermal properties. The addition of NAs affects the physical properties of HDPE by controlling the crystallization from the melt state. Specific NAs improve properties such as clarity, cycle time, and modulus. NAs are more widely developed for polypropylene (PP) than HDPE as its slower crystallization rate allows greater control in achieving property improvements. While certain NAs are effective in improving property characteristics in HDPE, greater control over the crystallization process would achieve further improvements in specific properties. Research has progressed in identifying effective NAs for HDPE, though the magnitude of the effects remains lower than those generally observed in PP. Inorganic and organic NAs are reviewed with an emphasis on the mechanisms by which they function. Fundamentals of polymer crystallization and modeling kinetics during both isothermal and nonisothermal studies provide the necessary framework for characterizing the effects of a NA in HDPE. Finally, the interactions between HDPE, NA, and industrial processing conditions as related to practical applications are discussed. **POLYM. ENG. SCI., 00:000–000, 2016.** **© 2016 Society of Plastics Engineers**

INTRODUCTION

In industrial applications, polymers are melted in processing steps such as extrusion and molding and the size, dimension, and distribution of crystalline domains, or crystallites developed upon cooling determine the final properties of the material. Specifically in high-density polyethylene (HDPE) with a density of 0.941–0.970 g/cc, often used in films, bottles, pipes, and tubes, optical, mechanical, thermal, and chemical properties are significantly affected by the crystallization process [1, 2]. Directed modification of the crystalline morphology during solidification from the melt state in HDPE can alter a wide range of physical properties such as water vapor transmission rate [3], optic clarity [3], shrinkage [4, 5], and cycle time in extrusion and molding [6, 7]. As these properties are directly related to the crystalline morphology of the polymer, directed modification to control the crystallization of HDPE can lead to significant improvements in targeted physical properties.

Crystallization occurs in two main stages known as nucleation and crystal growth [8, 9] During nucleation the polymer undergoes a phase change upon cooling where chains orient and align at the molecular scale into a periodic lattice. During crystal growth, polymer chains orient around the initial nucleation site, or nucleus, in a 3D pattern most often forming a spherical crystal cluster called a spherulite. At early stages of crystal growth, spherulites grow individually until they encounter other spherulites or the material interface, each defining a crystalline domain. Complete crystallization occurs when the crystalline and noncrystalline domains become space filling. The final material is characterized by the size and shape of these domains, often defined by the initial nucleation density and growth rate [9].

There are three classes of nucleation: (1) homogeneous nucleation or spontaneous nucleation; (2) self-nucleation; and (3) heterogeneous nucleation [9]. Homogeneous nucleation occurs in pure polymers due to the influence of supercooling also known as undercooling, which is the difference between the melt temperature (T_m) and the onset crystallization temperature (T_0) [10]. Self-nucleation is a result of partially melted polymer that provides structural heterogeneity, with the crystalline portion acting as a nucleus. Heterogeneous nucleation involves the addition of a foreign material that provides a seed upon which crystal growth can occur.

Nucleation and crystal morphology are affected by the addition of a nucleating agent (NA) that promotes heterogeneous nucleation. A NA is a dispersed material that acts as a local nucleus that is added to the polymer. As the ultimate physical properties of HDPE are strongly affected by crystal nucleation, growth, and final crystal morphology, the addition of NA provides a means to control the crystallization process and enable improvements in many physical properties [9, 11]. Thus, the interfacial properties of NAs often determine their effectiveness in seeding crystallization.

The addition of effective NAs in most polymers increases the rate of crystallization and the crystallization temperature, T_c. The increase in rate of crystallization and in T_c depends on the polymer/NA combination. However, there are limitations to the current effectiveness of NAs. Generally, NAs in HDPE cause a 1°–3° increase in T_c, a smaller crystallite size, and no substantial change in the fraction of the material that crystallizes. In contrast, nucleated PP for which crystallization behavior is more widely studied, increases in T_c trend up to 26° higher than for neat P [12, 13]. A beneficial result from the addition of effective NAs is reduced cycle times in polymer processing such as extrusion or molding. Fabricated parts solidify faster, increasing the rate of production. Another benefit is greater transparency or clarity in HDPE as NAs reduce crystal sizes to a range smaller than the wavelength of visible light to reduce light scattering [3]. Also, reductions in postinjection mold and postextrusion shrinkage values are achieved by the addition of a suitable NA due to a more uniform distribution of crystal sizes [14, 15].

Correspondence to: K. M. Seven; e-mail: kseven@dow.com
DOI 10.1002/pen.24278
Published online in Wiley Online Library (wileyonlinelibrary.com).

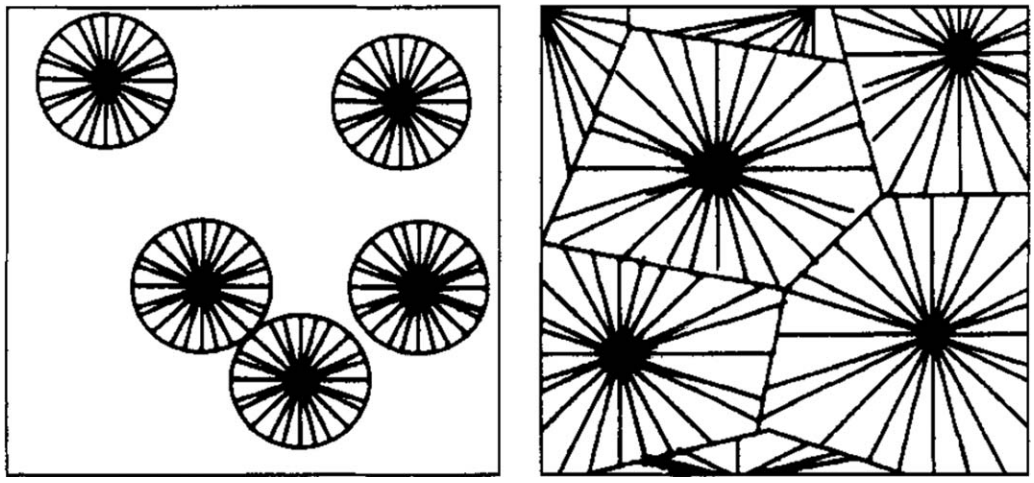

FIG. 1. Schematic representation of spherulite growth during initial stages (A) and final stages (B) of crystallization. (Reproduced from Ref 20, with permission from Elsevier).

Researchers comparing the effect of NAs on HDPE to their effect on polypropylene (PP) have concluded that nucleation in HDPE is more difficult to control than in PP due to HDPE's faster crystallization rate. PP's lower crystallization rate allows the NA more time to increase the nucleation density [16]. Relative to HDPE, the effects of NAs on PP crystallization have been widely researched and improved physical properties are well documented. The many effective NAs commercialized for PP are successfully used industrially to improve processing times, as well as the material properties of PP, which include optical clarity, warpage/shrinkage control, and modulus [17]. Compared to PP, relatively few commercially developed NAs are marketed for use in HDPE. Nevertheless, studies show that various organic and inorganic compounds are effective as NAs in HDPE. Effective NAs have the potential to achieve the same property improvements in nucleated HDPE as in PP though generally, to a lesser extent.

This article reviews the effects of NAs on the crystal formation process in HDPE and the resulting crystalline morphology. Critical polymer processing factors, such as cooling conditions, that control and affect the crystallization process and the resulting physical properties in HDPE are discussed. Flow-induced crystallization effects are briefly discussed but are not the focus of this article.

The techniques and mathematical models used to analyze HDPE crystallization kinetics are reviewed followed by a survey of the NAs investigated. Finally, this review summarizes the properties needed for designing effective NAs and potential new directions for material properties and processing conditions for achieving higher degrees of control of crystallization and nucleation in HDPE.

FUNDAMENTALS OF HDPE CRYSTALLIZATION

Crystallization in polymers leads to local alignment of the molecular chains into thin lamellae. Lamellae are formed from polymer chains that are folded back and forth in a regular pattern and the term lamella is often used interchangeably with crystallite [18]. The lamellae combine to form spherulites, which are spherically shaped clusters of crystallinity that grow radially from each nucleation point during crystallization. Within the spherulite are layers of oriented lamellae separated by noncrystallized amorphous regions [19]. Crystallization rates can be observed by measuring the growth of spherulites as a function of time using either optical microscopy or transmission electron microscopy (TEM) of thin sections. The isothermal radial growth of spherulites is typically linear as a function of time. Optical microscopy techniques show that spherulites continue to grow until they impinge on adjacent spherulites as shown in the second picture in Fig. 1 [20], creating a space-filling polycrystalline matrix [21].

Many beneficial physical properties such as higher modulus, higher tensile strength, and higher end-use temperatures of semicrystalline polymers such as HDPE can be attributed to crystal size distribution and degree of crystallinity, when compared to similar polymers that are mostly or fully amorphous. In contrast to fully amorphous polymers, the crystalline regions in semicrystalline polymers have a distinct melting temperature typically measured by differential scanning calorimetry (DSC).

Also above the glass transition temperature (T_g), and below the melting point, the modulus of a semicrystalline polymer is higher than that of a fully amorphous polymer, which is explained by the reinforcing effect of crystals in the polymer or locking in of the polymer structure caused by physical crosslinking of the amorphous regions by the crystallites or spherulites [10]. The crystallization process in polymers can only occur in the range of temperatures between the T_g and T_m of the polymer. The plot of temperature under isothermal conditions versus rate of crystallization takes the same basic shape shown in Fig. 2 for all semicrystalline polymers including HDPE. The characteristic shape of the curve in Fig. 2 is caused by the slowing of crystal growth with increasing viscosity at temperatures close to the T_g and by the reduced thermodynamic driving force as the melting point T_m of the polymer is approached. The rate of crystallization then peaks (T_p) at some temperature between T_g and T_m. The crystallization rates at both the T_g and T_m points are theoretically zero [10].

Crystallization in HDPE and in most semicrystalline polymers develops over time while cooling from the melt state. The general form of the curve is sigmoid shaped and is shown in Fig. 3 [10]. An initial induction time is required for the formation of spherulitic nuclei from the melt state. During primary

 DOI 10.1002/pen

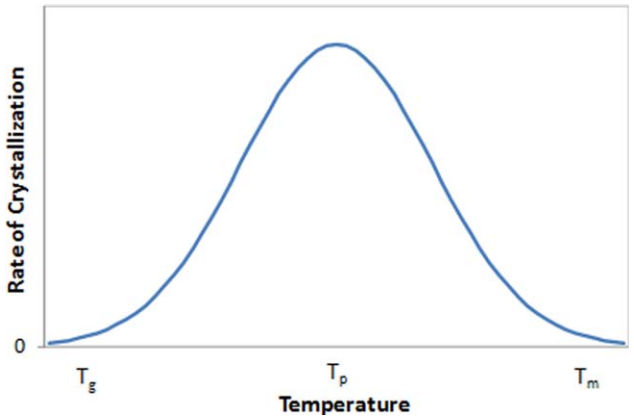

FIG. 2. Rate of crystallization versus temperature for semicrystalline polymers. (Reproduced from Ref. 10, with permission from Elsevier). [Color figure can be viewed in the online issue, which is available at wileyonlinelibrary.com.]

crystallization spherulites slowly form and then the crystallization process increases rapidly during which time the spherulites grow radially outward. Primary crystallization includes nucleation, crystal growth, and spherulitic organizing processes. Secondary crystallization occurs when crystallization slows due to the spherulites impinging on each other at which point the majority of the transformation is complete. During secondary crystallization, additional polymer chains may continue to move onto existing crystals and the crystallization may continue to increase although at a much slower rate. Secondary crystallization is typically more pronounced at higher cooling rates as there may be inadequate time for complete spherulite development during the primary crystallization phase and therefore further crystallization is shifted to the secondary crystallization phase [22]. Secondary crystallization can lead to additional shrinkage in finished molded or extruded parts in particular at temperatures greater than the T_g [19].

The general development of crystalline structure, which is described as crystalline fraction or degree of crystallinity as a function of time, is shown in Fig. 3. Both isothermally and nonisothermally crystallized polymers cooled at a constant rate roughly follow the shape shown in Fig. 3. However, extreme

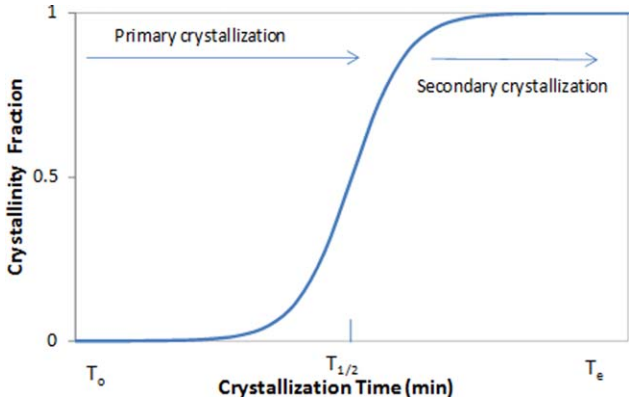

FIG. 3. Generalized curve for the degree of crystallinity versus time. (Reproduced from Ref. 20, with permission from Elsevier). [Color figure can be viewed in the online issue, which is available at wileyonlinelibrary.com.]

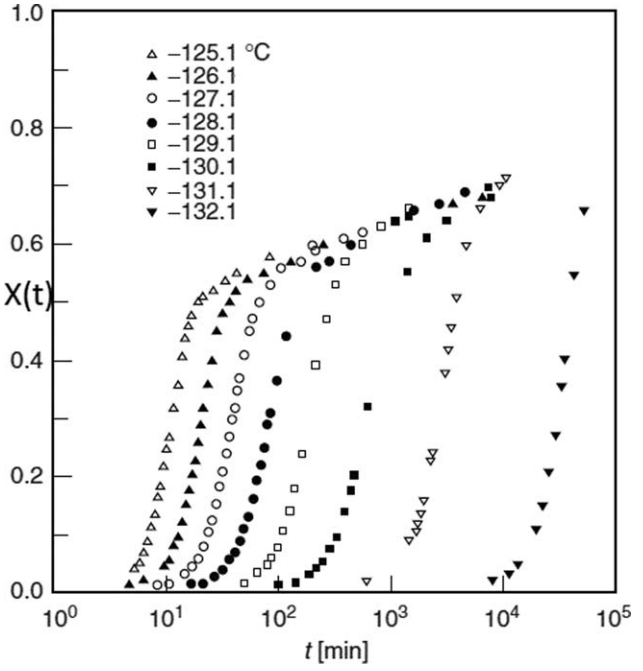

FIG. 4. Degree of crystallinity versus time for linear PE. (Reprinted with permission from E. Ergoz et al. [1] Copyright 1972 American Chemical Society).

nonisothermal conditions with high cooling rates (>5000°C/min) may distort the curve. The start of the crystallization or onset time of crystallization is T_0 in Fig. 3. The first portion of this curve before the sharp increase is often referred to as the induction time and is the time needed for the formation of nuclei. T_e is the time to reach complete crystallization. The crystallization half-time, $T_{1/2}$, is the time to reach 50% of the maximum attainable crystallinity [21]. Generally, most polymers including HDPE do not achieve complete crystallinity due to their semicrystalline nature. Figure 3 shows the normalized fraction of polymer crystallized versus time [23].

Polymer chains start out in a random coiled state and then undergo considerable reconfiguration to arrange into an ordered crystalline structure. The typical extent of crystallization for HDPE spans a broad range, roughly from 54 to 83%, depending on factors such as polymer branching, and the measurement method used to determine the value. The reconfiguration of the polymer chains into the crystalline structure is always obstructed to a certain extent by chain entanglements, polymer branches, and/or side groups. The formation of the crystalline structure in HDPE causes closer packing of polymer chains into the spherulite/crystal lattice structure, which leads to a change in density. Therefore, the change in density of the crystalline HDPE solid is proportional to the crystalline fraction [19].

As a general example of this phenomenon in polyethylene, Fig. 4 shows the actual measured degree of crystallinity development versus time for linear PE [1]. Generally, as T_c decreases from T_m a rapid increase in crystallization rate results as seen in Fig. 4. Also, the induction time becomes progressively longer as T_c increases. Independent of T_c, the curves show the same basic sigmoidal shape. Over time the same degree of crystallinity is achieved regardless of the crystallization temperature as long as it is above T_g and below T_m [1, 23].

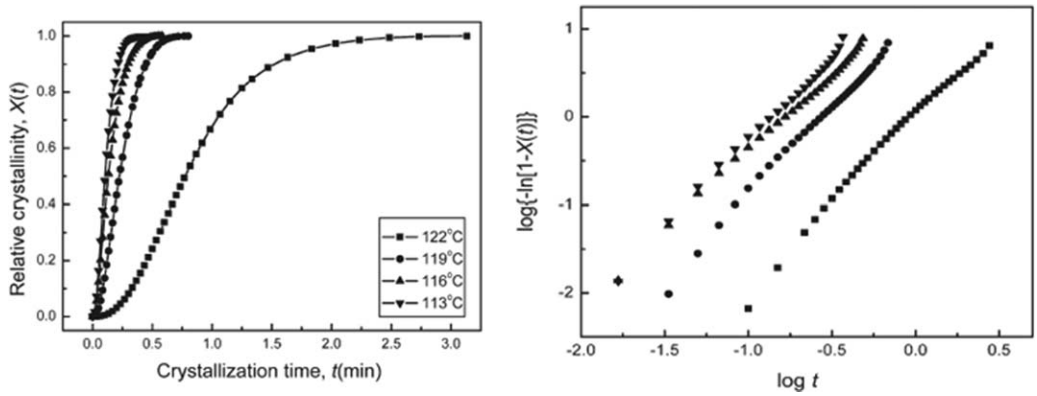

FIG. 5. Degree of crystallinity versus time for HDPE (A) and corresponding double logarithmic Avrami plot (B). (Reproduced from Ref. 26, with permission from John Wiley and Sons).

Both kinetic and thermodynamic elements promote the crystallization process. From a kinetic standpoint increased cooling or "undercooling" ($T_m - T_c$) promotes both the nucleation and crystallization process. From the thermodynamic standpoint, the crystal structure that forms is in a lower energy state than the melt state. A NA present in HDPE decreases the degree of undercooling needed to start the crystallization process and also leads to smaller spherulite sizes. The ultimate degree of crystallization achieved immediately after cooling to ambient temperature depends on the rate of crystallization and cooling rate [24]. As cooling rate increases especially for very rapid cooling conditions greater than 1000°C/min, a lower degree of crystallization is achieved. For instance, polymers subjected to rapid cooling in a cold mold in injection molding processes do not have adequate time to develop their full crystallinity. However. in the case of very rapid cooling to ambient temperature, the polymer will eventually reach the same level of crystallinity if maintained at temperatures between T_g and T_m; however, the process may take several weeks or months at ambient temperature which is not a practical time scale [1, 19]. Cooling rates also have a significant effect on the time to start the crystallization process as typically observed in nonisothermal crystallization studies. The general trend seen in DSC cooling curves is that crystallization starts at higher temperatures when the cooling rate is lower because there is more time at higher temperatures for the nuclei to start the nucleation process and begin crystallization. Conversely, higher cooling rates delay nucleation activity as there is insufficient time to initiate the crystallization process at higher temperatures and therefore the nucleation occurs predominantly at lower temperatures.

ISOTHERMAL CRYSTALLIZATION KINETICS AND THE AVRAMI EQUATION

The determination of the relative crystallinity $X(t)$ as a function of time at a constant temperature can be used to analyze isothermal crystallization kinetics in polyethylene. The relative crystallinity at time t is defined in *Eq. 1* and has a maximum value of 1 and minimum value of 0 [25].

$$X(t) = \frac{X_c(t)}{X_c(t_\infty)} = \frac{\int_0^t \frac{dH}{dt}\,dt}{\int_0^\infty \frac{dH}{dt}\,dt} = \frac{\Delta H_t}{\Delta H_\infty}, \quad (1)$$

where H_t is the heat generated through time t, H_∞ is the total heat generated to the end of the crystallization process, $X_c(t)$ is the crystallinity at time t, and $X_c(t_\infty)$ is the crystallinity at the end of the crystallization process [26]. This equation enables a convenient analysis of crystallization based on calorimetry experiments using a DSC. The overall crystallinity is the percentage of the measured heat of fusion compared to the theoretical heat of fusion of the pure polymer [9]. Two additional techniques for measuring relative crystallinity include density and wide-angle X-ray scattering (WAXS). The density method is calculated based on tabulated density values for the amorphous and crystalline phases along with the measured density of the polymer. In X-ray diffraction the crystalline regions in the polymer produce sharp diffraction peaks whereas the amorphous regions produce broad halos. The degree of crystallinity can be estimated by integrating the relative intensities of the peaks and halos [9, 27].

The Avrami *equation* (*2*), first published in 1939 and still used successfully today, describes the isothermal crystallization kinetics of many semicrystalline polymers including HDPE. Several examples of HDPE blends analyzed by the Avrami method are included in this article [28–30]. The equation describes how solids transform from one state of matter or phase to another at constant temperature and can also describe some types of chemical reactions [25].

$$X(t) = 1 - \exp\,(-Kt^n), \quad (2)$$

where $X(t)$ is the time-dependent relative crystallinity, n is the Avrami exponent, K is the Avrami rate constant involving nucleation and growth parameters, and t is the crystallization time. The Avrami exponent n depends on the type of nucleation and growth process. Generally the values of n are between 1 and 4 [28–30].

The Avrami equation takes the following assumptions into account: (1) that the nucleation process occurs randomly in space; (2) that time dependence of nucleation is either zero or first order as described below; and (3) crystals have a specific geometric form. Both assumptions 2 and 3 are described by the n value [20].

The value of the Avrami exponent n is composed of two terms N and C where $n = N + C$ [31]. The Avrami equation includes both instantaneous nucleation where nuclei develop at once on cooling the polymer to the crystallization temperature called zero-order where $N = 0$ and first-order sporadic nucleation where the number of nuclei formed increases linearly with

 DOI 10.1002/pen

time where $N = 1$. However, in many cases the nucleation process falls somewhere between the completely instantaneous and completely sporadic cases and the result is a noninteger Avrami index [31]. The typical value of n for polyethylene is 2.6–4.0 [20]. The value of n often decreases as the crystallization proceeds [32]. The geometric shape of the crystals also influences n, where C is the dimension of the growth. For 3D spheroidal growth, 2D planar discoidal growth, and 1D rod growth, $C = 3$, 2, and 1, respectively. It is common for $n = 4$ where nucleation is first order and the growth dimension is spherical.

Equation 2 is typically rearranged in a linear form and a double logarithm applied:

$$\log[-\log(1-X(t))] = n\log t + \log K. \tag{3}$$

A typical example of an isothermal relative crystallinity curve for a HDPE sample is shown in Fig. 5A. The sigmoid-type curves typically shift to the right with increasing isothermal crystallization temperature and the crystallization rate slows down [26].

If *Eq. 3* adequately describes the isothermal crystal kinetics of the polymer then the plot of $\log[-\log(1 - X(t))]$ and $\log t$ is a straight line and the values of n and K can be obtained from its slope and intercept, respectively. An example plot is shown in Fig. 5B for HDPE based on the data shown in Fig. 5A [26]. For the Avrami equation to successfully describe the kinetics in the system the data points in this plot must be highly linear within a specific conversion range with a very high correlation coefficient [31]. The Avrami equation adequately described the primary crystallization kinetics in the isothermal study of the barium sulfate NA system. However, the authors commented that the plots tend to deviate from linear behavior in the later stages of crystallization due to the effect of secondary crystallization. A similar nonlinear behavior occurred in the Avrami kinetic studies of UHMWPE as NA [33, 34].

In some cases the data may fit a straight line over a smaller range of crystallization conversions often around the 50% area. In this case, some improvements in the data fit may be achieved by assigning a noninteger value of n because samples may not have the same consistent geometry of rod, disc, or sphere throughout their volume and a combination of zero- and first-order nucleation may be present. Grenier and Homme [35] published a review of the limiting factors for applying the Avrami equation. Below, examples of crystallization kinetics analysis using the Avrami equation are included in the Nucleating Agent Developments section.

NONISOTHERMAL CRYSTALLIZATION KINETICS

Often research on polymer crystallization is conducted under idealized isothermal conditions, which greatly simplifies the mathematical analysis but fails to account for the varying cooling rates and temperatures typically encountered within the polymer in applications. However, the study of crystallization in an environment with continuously changing temperatures is of greater practical importance as industrial processes generally occur under nonisothermal conditions [10].

One of two models presented by Ziabicki et al. [36, 81] describes the nonisothermal crystallization of polymers as a sequence of isothermal steps. The Ziabicki equation is a series expansion of the Avrami equation thus having limited effectiveness because it is restricted to temperature ranges where experiments measure isothermal crystallization [36].

Nakamura et al. [10] published a detailed study of the nonisothermal crystallization kinetics of neat HDPE. This study utilized incident X-rays scattered from an HDPE film sample inside a special sample holder with heating stage and thermocouple to monitor changes in crystalline diffraction peaks versus temperature during cooling. The degree of crystallinity $X(t)$ is calculated by comparing the diffraction peak intensities at time t to the completely amorphous and completely crystalline states. These in situ experimental results obtained for nonisothermal crystallization agreed with the theoretical predictions calculated from the Nakamura equation. The Nakamura equation assumes instantaneous nucleation [37, 38].

As derived, the Avrami equation applies only to isothermal crystallization. Jeziorny [39] modified the Avrami equation to describe the kinetics of nonisothermal crystallization. A corrected form of the rate term (K) used in the Avrami equation assuming a constant cooling/heating rate was proposed. The relative crystallinity at a set cooling rate (R) is a function of the crystallization temperature (T) and rewriting *Eq. 1*: [40]

$$X(t) = \frac{\int_{T_0}^{T_c} \frac{dH}{dT}\, dT}{\int_{T_0}^{T_\infty} \frac{dH}{dT}\, dT}\ , \tag{4}$$

where $X(T)$ is the relative crystallinity as a function of crystallization temperature. The crystallization onset temperature is T_0 and T_c and T_∞ represent the crystallization temperature at time t and after the completion of the crystallization process. The crystallization time variable t can be obtained using:

$$t = \frac{T_0 - T_\infty}{R}\ , \tag{5}$$

where R is the cooling rate in °C/min. The rate of nonisothermal crystallization depends on R, and K can be corrected to obtain the primary rate constant K_r:

$$\log K_r = \log K/R. \tag{6}$$

Jeziorny theory was used to model the nonisothermal crystallization kinetics in both SiO_2 and TiO_2 NA studies. An acceptable linear fit of the data was achieved with this model in both systems except at the very end stages during secondary crystallization [33, 34].

Ozawa modified the Avrami equation for nonisothermal crystallization assuming that the polymer was heated or the polymer melt was cooled at a constant rate. According to the Ozawa theory, the Avrami equation becomes *Eq. 7*, which is called the Ozawa equation. The Ozawa equation is based on both temperature and cooling rate R:

$$X(t) = 1 - \exp\left[-\frac{K(T)}{R^m}\right], \tag{7}$$

where $K(T)$ is the cooling or heating temperature function, m is the Ozawa exponent which depends on the dimensions of the crystal growth and order of nucleation.

Taking the double-logarithmic form:

$$\log[-\log(1-X_t)] = \log K(T) - m\log R. \tag{8}$$

Measuring a crystallization process at different cooling rates and plotting $\log[-\log(1 - X_t)]$ against $\log R$ at a given temperature, straight lines should be obtained if the Ozawa method is

valid. The parameters m and K (T) can be determined from the slope and intercept, respectively.

Eder and Wlochowicz [41] showed that the Ozawa method did not produce straight lines in the $\log[-\log(1-X_t)]$ versus $\log R$ plot for HDPE indicating that this model was not adequate, which was also confirmed by Liu et al. [42]. Likewise, attempts to utilize the Ozawa method in the SiO_2 and $CaCO_3$ NA systems showed unacceptable nonlinear behavior in both the neat HDPE and composites during both primary and secondary crystallization phases [34, 43]. In all cases, this discrepancy was attributed to factors neglected in the Ozawa theory including secondary crystallization and dependence of lamellar thickness on the T_c. The Ozawa theory also does not include variability of n with T_c. Slow or secondary crystallization in PE can sometimes be greater than 40% of the total crystallinity [41].

To achieve a better description of the crystallization behavior, Mo and coworkers [42] proposed combining *Eqs. 2* (Avrami equation) and [7] (Ozawa equation). The combination provides a relationship between cooling rate R and crystallization temperature T.

$$\log(K) + n\log t = \log K(T) - m\log R \tag{9}$$

can be rewritten as

$$\log R = \log F(T) - a\log t \tag{10}$$

The parameter $F(T)$ is the heating or cooling rate: $F(T)=[K(T)/Kt]^{1/m}$ and a is the ratio of the Avrami exponent n to the Ozawa exponent m or $a = n/m$. Mo's method was successful in describing the nonisothermal kinetics at both lower and higher degrees of crystallinity ($X > 0.8$) for TiO_2, SiO_2, and $CaCO_3$ and overall a better linear fit was obtained in comparison to the Jeziorny and Avrami methods [33, 34, 43].

ACTIVATION ENERGY

One way to interpret the mechanism of heterogeneous nucleation is the active NA reduces the interfacial free energy between crystalline polymer and the NA constituent as compared to the polymer–polymer crystalline-amorphous interfacial energy. The activation energy or ΔE is the energy to transport molecular chains from the molten state to the crystal growth surface [44]. The reduced interfacial free energy decreases the activation energy for nucleation, thus lowering the amount of cooling required. As temperature is lowered, the drive to crystallization is favorable until the increase in polymer viscosity inhibits the chain alignment, making the crystallization process more difficult at low temperatures [45].

Binsbergen's study of polyolefin crystallization supports this theory, showing a greater tendency of the HDPE crystallite to adsorb the foreign material rather than the liquid (melt) phase because of reduced interfacial energy thereby lowering the activation energy required for nucleation [46].

To estimate the activation energy in nonisothermal systems, Kissinger [47] relates the maximum rate of extent of conversion to activation energy, ΔE, while cooling [34].

$$\frac{d[\log(\frac{R}{T_p^2})]}{d(\frac{1}{T_p})} = -\frac{\Delta E}{G}, \tag{11}$$

where G is the universal gas constant, T_p is the peak crystallization temperature at maximum crystallization rate, and R is the cooling rate, dT/dt. This equation allows comparison between experiments conducted at various cooling rates [42]. Other examples of this type of activation energy calculation are presented in the Nucleating Agent Developments section.

Another method to estimate ΔE utilizes the Friedman equation.

$$\ln\left(\frac{dX_t}{dt}\right) = \text{constant} - \frac{\Delta E}{RT}.$$

The instantaneous crystallization rate as a function of time is dX_t. The constant is an empirical pre-exponential factor. Plots of dX_t/dt versus $1/T$ yield a straight line with slope equal to $-\Delta E/R$ [33, 43].

HOMOGENEOUS NUCLEATION AND HDPE MOLECULAR WEIGHT FRACTIONS

Before considering the effects of NAs in HDPE it is useful to discuss the most basic form of crystallization in HDPE which involves homogeneous nucleation. The average molecular weight (M_w) and molecular weight distributions of HDPE influence its nucleation and crystallization. Generally, an increase in M_w results in higher viscosity slowing the process by which the chains move into an ordered crystalline structure during cooling, and thus lowering the crystallization rate.

For instance, studies conducted on PP copolymers with a range of melt flow index (MFI) showed that the crystallization rate and level of crystallinity increased with decreasing M_w or viscosity, or increased MFI. Similar trends would be expected for HDPE. Physical properties of PP, such as crush resistance and shrinkage, were improved with increased MFI polymers. The improved crush resistance was attributed to increased levels of crystallinity in the higher MFI polymers [48].

Chiu and Fu [49] studied the effect of various HDPE M_w fractions on the crystallization kinetics and related crystal morphology by utilizing DSC, TEM, X-ray scattering, and other techniques. Results confirmed that M_w affects the crystallization rate, Avrami exponent, and crystal morphology. Generally, the lower M_w samples showed higher crystallization rates under identical T_c and conditions. As expected, based on crystal growth theory the crystallization process was faster for the samples crystallized at lower T_c (higher ΔT) regardless of M_w. The authors hypothesized that the nucleation mechanism changes from spontaneous to sporadic nucleation as T_c increases. This conclusion is supported by polarized optical microscopy (POM) images taken of low and high M_w samples at differing T_c values [49].

POM micrographs of the low M_w samples crystallized from the melt state to room temperature showed considerably different morphologies as compared to the high M_w samples with $M_w > 5800$. The samples with $M_w > 5800$ had a higher density of nuclei which led to smaller spherulites as compared to spherulite sizes in the lower M_w samples [49].

NUCLEATING AGENT DEVELOPMENTS

Classes and Characteristics of NAs

While there is no method for a priori prediction of the performance of a NA for a particular polymer, previous studies led

DOI 10.1002/pen

TABLE 1. Summary of effective nucleating agents for HDPE.

Category	Nucleating agent	Reference
Nanoscale/ inorganic fillers	Calcium carbonate	43, 51
	Titanium dioxide	33
	Barium sulfate	26
	Silicon dioxide	34
	Expanded graphite	52, 53
	POSS	25, 54
	Multiwall carbon nanotubes (MWNT)	55–57
	Montmorillonite clay	32
	Vermiculite nanocomposite mineral	58
	Talc	14
	Haloysite nanotubular clay	59
Organic fillers/ additives	Ultra high-molecular-weight PE	4
	Sisal fibers	60
	High-modulus PE fiber	61
	1,2-Cyclohexanedicarboxylic acid, calcium salt:zinc stearate[a]	62, 63
	Anthracene	64
	Pottasium hydrogen phthalate	46, 64
	Benzoic acid type compounds	12, 65
	Sodium benzoate type compounds	12
	Disodium bicyclo[2.2.1]heptane-2,3-dicarboxylate[b]	66
	1,3:2,4-bis(3,4-dimethylbenzylidene) sorbitol[c]	66
	Zinc monoglycerolate[d]	67

POSS, polyhedral oligomeric silsesquioxanes.
[a]For example, Hyperform™HPN-20E.
[b]For example, Hyperform™ HPN-68L.
[c]For example, Millad™ 3988.
[d]For example, Irgastab™ 287.

researchers to identify common characteristics of the more effective NAs [12, 50]. Prior to crystallization these NAs are typically insoluble in the melt with a higher T_m than the polymer. These NAs are often crystalline materials with preferably similar crystalline structure to the polymer. The complementary registry enables epitaxial crystallization on the NA surface [12]. Effective NAs frequently have both polar and nonpolar attributes, such as salts of benzoic acid which have nonpolar benzene rings that align in parallel layers or rows that interface with the polymer chains. These salts of benzoic acid can form an alternating polar and nonpolar layered structure, with the nonpolar portion in close contact with the polymer melt. NAs for HDPE are divided into inorganic and organic types as shown in Table 1. The list of NAs in Table 1 is not exhaustive but does include the most commonly researched and reported NAs proven effective for HDPE. Whether inorganic or organic, the effectiveness of the NA is determined by measuring the T_c on cooling in a nucleated HDPE sample. A higher T_c value indicates faster crystallization and, therefore, a more effective NA. Each NA listed in Table 1 includes one or more of the common characteristics stated above. Other properties such as geometrical form, optimum particle size, and surface morphology can increase the effectiveness of the NA. Finally, the NA must be well dispersed within the polymer melt to maximize its effectiveness [16, 46]. Examples of these effects are discussed further in the next sections.

Effect of NA Concentration and Crystallization Temperature

Studies of NAs in HDPE frequently address whether the concentration of the NA impacts performance, as measured by the increase in T_c and crystallization rate indicating a more effective NA [12, 68, 69]. For the NAs listed in Table 1, the underlying studies that address concentration include the NA ranges from 0.5 to 5 wt% while the other studies use a fixed amount of the NA that is generally within that range. The NAs in Table 1 all show an increase in T_c and crystallization rate at all NA concentrations studied in HDPE. Those studies of NAs in HDPE that include the effect of concentration show that the performance of the NA is concentration dependent. For example, studies of NAs listed in Table 1, including UHMWPE [4], $CaCO_3$ [43], TiO_2 [33], SiO_2 [34], $BaSO_4$ [26], POSS [25], graphite [52], MWNT [55], and ionomer-treated sisal fibers [60], correlate performance with the amount of the NA in the HDPE. It is therefore presumed that concentration-dependent behavior is the norm rather than the exception. Of course, there must be limitations to this trend as product properties increasingly depend on the composite nature of these materials at higher concentrations, causing the additional amount of NA to have diminishing returns at high loading.

In some studies the concentration of NA necessary to achieve the largest increase in T_c and crystallization rate was determined. For example, Song et al. [4] showed with plots of crystallization time versus X_t that the crystallization rates of the composites vary with the concentration of UHMWPE. The sample with 3 wt% UHMWPE had both the highest crystallization rate and the shortest time to reach maximum relative crystallinity. As the level of UHMWPE was gradually increased from 0.5 to 3 wt% the crystallization rate continued to increase as shown in Fig. 6, with the crystallization rate highest for 3 wt%. However, as the 3 wt% concentration is approached the increases in crystallization rate become less and less significant. Based on these results the authors conclude that above 3% no significant increases in crystallization rate would be expected [4].

Similarly, Minkova and Mihailov studied the nonisothermal crystallization kinetics of blends of HDPE with UHMWPE as a function of blend composition, demonstrating effectiveness of 30 wt% of UHMWPE; both HDPE and UHMWPE crystallization rates were found to be higher than their corresponding neat systems [70, 71].

A maximum crystallization rate was determined in an isothermal study of POSS, which included a concentration range of 5–10 wt% of POSS in HDPE. The maximum crystallization rate was determined to be 1 wt% as determined by measuring $T_{1/2}$ values by DSC [25]. However, a different concentration dependence of POSS versus T_c was found in a separate study under nonisothermal conditions, which showed that only a sample with 10 wt% POSS had significant increases in T_c. This highlights issues in comparing various systems and techniques, in particular the range of results possible when studying crystallization under isothermal and nonisothermal conditions [54].

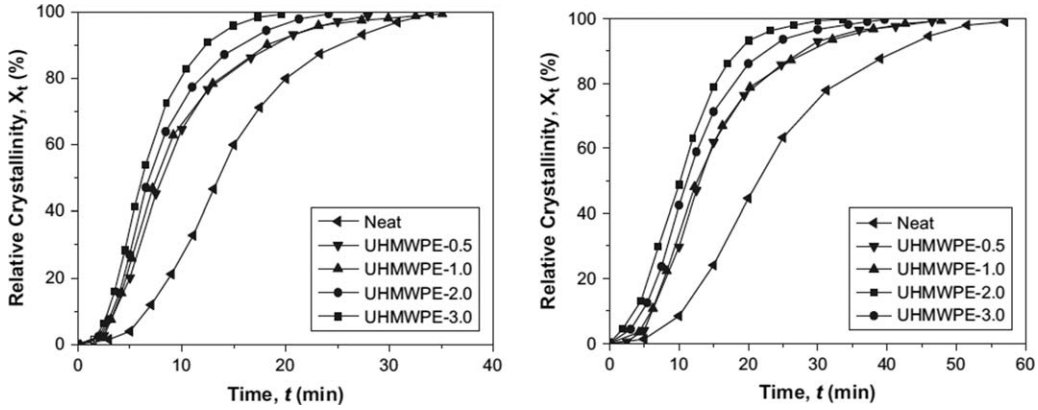

FIG. 6. Plot of relative crystallinity of UHMWPE/HDPE composites at (A) 121.5°C and (B) 122.0°C isothermal crystallization temperatures. (Reproduced from Ref. 4, with permission from Elsevier).

Reduced Degree of Crystallinity

In most studies, a reduction in overall crystallinity as a function of increasing NA concentration was reported as compared to neat HDPE. Typically although with a few exceptions, the crystallinity decreases as the NA concentration increases as compared to the neat HDPE. The reduction in crystallinity is explained by the competing effect of reduced polymer chain mobility in the presence of a NA. The particles can impede or confine the mobility of polymer chains making it more difficult for the chains to arrange themselves into the ordered crystal structure. Generally, the free volume of the polymer chains is reduced as the NA content increases, which leads to decreased polymer chain motion. The confined motion of the chains can cause a slight reduction in crystallization rate particularly as the loading of the NA is increased above the optimum level for NA effectiveness [50]. For example, this effect was reported to occur with $CaCO_3$ and the reduced crystallinity was confirmed by DSC and wide angle X-ray diffraction (WAXD) curves. The crystallinity of the simple blend of HDPE with 5 wt% $CaCO_3$ showed a reduction in crystallinity as compared to the neat HDPE. However, further reductions in crystallinity were obtained in a sample containing a maleic anhydride PE (manPE) compatibilizing agent with a HDPE/manPE system blended also with 5 wt% $CaCO_3$. The authors hypothesized that the manPE compatibilizer leads to increased interaction between the HDPE chains and $CaCO_3$, which increases the confinement of the polymer chains [43]. Similar reductions in crystallinity with increasing NA amount were determined in studies with TiO_2 [33], expanded graphite (EG) [52], and MWNTs [72].

In contrast, the percent crystallinity of the HDPE portion of an HDPE/sisal fiber composite increased significantly as the amount of sisal fiber in the HDPE increased. However, the crystallization enhancement may be different at the fiber/polymer interface as compared to the bulk of the matrix. This result was contrary to typical studies of NAs in HDPE in which a decrease in crystallinity of the HDPE fraction is measured with increasing filler content [60].

The change in crystallinity due to the presence of NAs correlates to changes in ΔH_m, which is the enthalpy change during melting. These changes are reflected in X_c or ΔH_m both measured by DSC. Studies of NAs such as $CaCO_3$ [51], SiO_2 [34], graphite [52], and TiO_2 [33] showed lower X_c results, while sisal fiber composites showed higher X_c as reflected in higher ΔH_m [60]. In some studies involving POSS [25] and $BaSO_4$ [26], crystallinity measurements were not included and therefore no conclusions could be determined regarding this effect for those NAs.

The effect of MWNTs in one study showed only slight differences in degree of crystallinity that were not considered significant by the authors [55]. However, in another study conducted under different conditions the MWNTs showed a decrease in crystallinity with increasing MWNT concentration [72]. The concentration effect of UHMWPE as NA on degree of crystallinity was too small to be considered significant. The UHMWPE samples with 0.5, 2, and 3 wt% levels showed about 1% reduction in crystallinity as compared to the pure HDPE [4].

The Effect of NAs on Crystal Morphology and Structure

The focus here is mostly on the crystal morphology which refers to the external form or shape of the crystal in the macroscopic scale, whereas crystal structure refers to the molecular or atomic level of order within the crystal [8]. Crystallization kinetic studies as indicated by n often show that the addition of NAs does not change the crystalline morphology of HDPE. For example, in SiO_2 [34] and TiO_2 [33], n did not change significantly in the nucleated versus pure HDPE, indicating that the geometry or mechanism of HDPE crystallization did not change [33]. Contrary to this result sisal fibers showed significantly higher n of about 3 in composite samples as compared to the pure HDPE which showed an n value of about 2 [60].

WAXD is another tool used to characterize changes in crystalline structures in HDPE upon addition of NA. For example, WAXD of the TiO_2 [33], $CaCO_3$ [43], carbon nanotube (CNT) [56], and $BaSO_4$ [26] NA studies showed no change in crystal structure. However, the lamellar thicknesses can change, which is related to the size of the particular crystal morphology rather than structure. In some studies, WAXD was also used to measure lamellar thickness. For example, WAXD showed that the lamellar thickness increased in both TiO_2 and $BaSO_4$ composite samples. Increased lamellar thickness in nucleated composites corresponds to higher enthalpy change or ΔH_m as compared to the pure HDPE at the same cooling rates [33, 43].

Lamellar thickness typically increases in nucleated samples as compared to the pure HDPE. Some studies include results of

 DOI 10.1002/pen

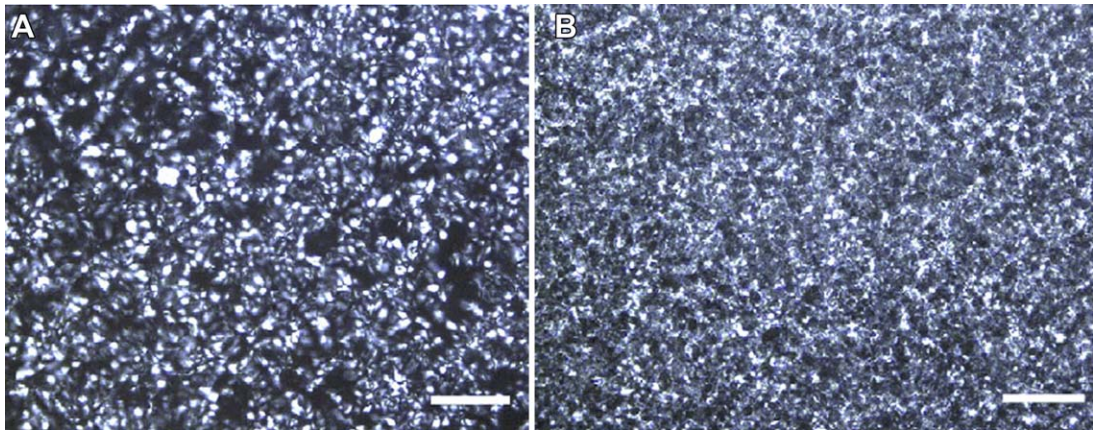

FIG. 7. Crystal morphology of neat HDPE (A) and HDPE/UHMWPE (B) composites after 50 min at 129°C. The white bar is 50 μm. (Reproduced from Ref. 4, with permission from Elsevier). [Color figure can be viewed in the online issue, which is available at wileyonlinelibrary.com.]

T_m values of nucleated versus non-nucleated samples. For example, $BaSO_4$, UHMWPE, and CNTs as NAs showed higher T_m than pure HDPE, which indicated that the NA caused thicker crystals or more perfect crystals to form as compared to the pure HDPE [26, 56]. Contrary to this result both graphite and SiO_2 showed a 2° and 5° decrease in T_m, respectively, compared to pure HDPE, indicating increased crystal imperfections due to the presence of the NA [34]. The T_m values of $CaCO_3$ [43] and MWNT [55] showed no significant changes in T_m versus the neat HDPE.

Spherulite Size and Number

Early studies in the 1970s utilized a microscopy technique to evaluate the nucleating effect of roughly 2000 compounds on polyolefins. While the testing focused on PP, substances active in PP were often active in other polyolefins such as HDPE. The method involved observing the size and number of spherulites in the crystallizing mixtures. The results showed that a good NA reduced the spherulite diameters by 1/10 to 1/5 as compared to the spherulite diameters in the non-nucleated polymer. Binsbergen [46] showed that the number of active seeds is strongly temperature dependent.

The modern microscopy technique used to study the crystallization process utilizes POM and a hot stage to allow real-time capture of the crystallization process at selected temperatures [4]. For example, POM was used to study the crystallization process of neat HDPE and 3 wt% UHMWPE composites at 129°C at selected time intervals as shown in Fig. 7. Figure 7 shows the POM results after 50 min of crystallization time at 129°C. The POM results provided further confirmation of the much faster crystallization rate of the composite sample with 3 wt% UHMWPE showing more nuclei versus neat HDPE at a given time interval. These results showed that the spherulites in the UHMWPE composite were much smaller than those in the neat HDPE [4]. The POM technique was also utilized in the TiO_2 and $CaCO_3$ studies and showed similar increases in the number of nuclei and smaller spherulite sizes and these results are presumed to occur to some extent with all effective NAs [33, 43].

Spherulite growth rates typically increase in samples with NA as compared to the pure polymer and growth rate is inversely proportional to $T_0 - T_c$. For example, the spherulite growth rate increased in an HDPE/$CaCO_3$ sample compared to the neat HDPE, which corresponds to an increased rate of crystallization [51].

The Effect of NA Particle Size and Particle Surface

Nanosized particles can in principle produce higher efficiency of nucleation as lower concentrations provide a higher number of available nucleating sites due to the increase in surface area to volume ratio for decreasing particle size [73]. Nanoparticles are different from typical reinforcing agents used in polymers in that the nanoparticle is capable of interacting with the polymer on a molecular level due to its small size and high surface area. Nanoscale NAs are added at low concentrations, typically 1–3 wt%. However, under certain conditions and concentrations, a reduction in mobility of the molecular chains can occur which reduces crystal growth rate and NA effectiveness [25, 43]. For example, studies involving both EG and untreated graphite (UG) have shown that particle surface area has an effect on the NA performance independent of surface chemistry [52, 53]. At 10 wt%, a larger increase in T_c occurred with the EG than with the UG as compared to the neat HDPE. The authors concluded that the higher surface-to-volume ratio of the EG as compared to UG in the HDPE matrix led to a higher number of nucleation sites. The higher surface-to-volume ratio may yield better interaction between crystalline HDPE and graphite [52].

Typically inorganic NA studies describe changes that are made to the NA particle surfaces. The surface coating or lack of surface coating on NAs such as $CaCO_3$ affects the crystallization of HDPE. In one study a precipitated $CaCO_3$ with no stearic acid surface treatment acted as a NA whereas stearic acid-treated $CaCO_3$ did not [74]. The SiO_2 study utilized a silane coupling agent to modify the particle surface; however, the study did not focus on how the surface changes affected the NA performance [34]. In another study, $BaSO_4$ particles were treated with sodium stearate as this treatment is widely used to improve the dispersion and toughness in the matrix as compared to untreated particles [26]. Without systematic study, it was presumed that the treated $BaSO_4$ particles would function better as NAs as compared to untreated particles. Sisal fibers were treated

with an ionomer coupling agent in order to improve fiber–matrix bond strength and improve the reinforcement effects of the sisal fibers in the matrix. The NA effectiveness of these particles was determined; however, the study did not focus on how the changes to the particle surface affected the NA performance [60].

The Effect of NA Dispersion

Effective dispersion of the NA in HDPE is critical to maximizing its effectiveness [16, 46]. Huang et al. [43] studied nonisothermal crystallization of neat HDPE, HDPE/$CaCO_3$, HDPE/maleic anhydride (man), and HDPE/manPE/$CaCO_3$ composites. The manPE is a maleic anhydride-modified material which acts as a compatibilizing additive for the $CaCO_3$ in the HDPE. DSC results showed that the HDPE/manPE/$CaCO_3$ sample had the highest T_0 and T_p values of all the samples. The authors hypothesize that the increased compatibility caused by the manPE produced better overall $CaCO_3$ particle dispersion in HDPE, which led to an increased number of effective nucleating particles [43].

X-ray diffraction and TEM studies with POSS as a NA showed that crystalline aggregates start to form at concentrations above 1wt%. These aggregates did not effectively promote the crystallization process or nucleation activity, resulting in constant n values at >1 wt% POSS. The authors showed that only well-dispersed POSS affects the crystallization mechanism and the rate of crystallization of the HDPE matrix and acts as a NA [25].

CNTs are commonly known to be difficult to disperse and studies have shown that only well-dispersed CNTs can function as effective NAs [56]. Vega et al. [55] studied nanocomposites of HDPE melt mixed with an in situ polymerized HDPE/multiwall carbon nanotube (MWNT) masterbatch. The nanocomposite was studied under isothermal conditions containing 0.52wt% MWNT. The in situ technique was utilized to prevent CNT aggregation and optimize dispersion in the final composite and results from simple melt blended systems may differ significantly. Trujillo et al. [56] showed that simple melt blended incorporation of MWNTs into HDPE had poor dispersion and did not form crystals with higher T_m and the crystal lamellae were thinner as compared to the in situ produced composites. He et al. [72] completed a similar study but used a solution method to crystallize the HDPE onto MWNTs to overcome the poor dispersion problem. The method involved cooling and crystallizing dissolved HDPE from hot *p*-xylene with a controlled amount of dispersed MWNTs [72].

Activation Energy

Most studies with a few exceptions confirm that NAs cause a reduction in activation energy necessary for nucleation. For example, with $CaCO_3$ the activation energies, estimated using the Friedman equation, were lower as compared to the neat HDPE at the same relative crystallinity. The composite with only $CaCO_3$, as mentioned above promoted more spherulite nucleation on the $CaCO_3$ surface than the $CaCO_3$/HDPE blend with maleic anhydride compatibilizer [43]. This effect is also evident in TiO_2 used as NA, comparing anatase and rutile phases of TiO_2. The plot of crystallization activation energy of neat HDPE and HDPE/TiO_2 composites, as determined by the Friedman equation, is shown in Fig. 8 as a function of X_t. The HDPE/TiO_2 composites all show lower activation energy at any given X_t, demonstrating that TiO_2 promotes the crystallization of HDPE. The HDPE/anatase TiO_2 blend has the lowest activation energy. The results shown in Fig. 8 suggest that the HDPE becomes more difficult to crystallize toward the end of the process as activation energy tends to level out at roughly 60–90% X_t. The $CaCO_3$ NA shows similar trends in activation energy [33, 43].

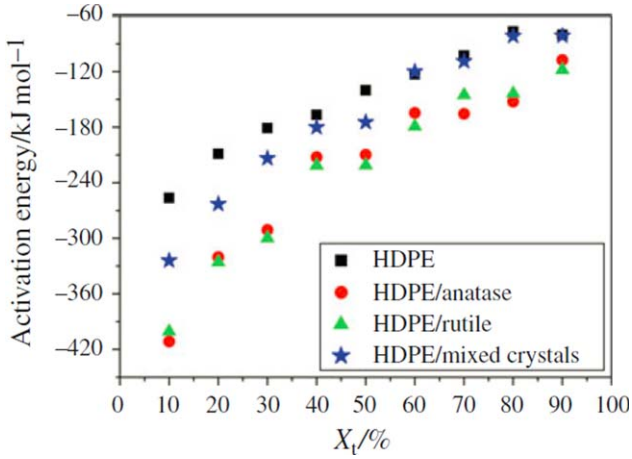

FIG. 8. Nonisothermal crystallization activation energy of neat HDPE and HDPE/TiO_2 composites. (Reproduced from Ref. 33, with permission from Springer). [Color figure can be viewed in the online issue, which is available at wileyonlinelibrary.com.]

PRACTICAL APPLICATIONS

Much of the published information on use of NAs in HDPE is found in the patent literature, rather than textbooks and journals. The patent literature describes practical industrial applications of NAs in HDPE in which the addition of certain NAs improved film clarity and haze, increased modulus, improved barrier properties, reduced shrinkage, warping, and sag in extruded and molded parts, and reduced polymer processing times in molding and extrusion operations. Several representative examples are detailed below.

UHMWPE can prevent sag in large pipe extrusion processes using PE-100 bimodal HDPE resin as well as improve production cycle time by decreasing the solidification or crystallization time [4]. Nonuniform cooling of the inside versus outside surfaces of pipes during extrusion leads to internal stresses. In normal pipe production water is used to rapidly cool the inside and outside of the pipe which causes differing cooling gradients within the pipe wall. This uneven cooling causes stresses within the wall of the pipe due to slower crystallization and nonuniform shrinkage in those regions. It is commonly known in the pipe industry that higher crystallization rates are favorable for eliminating or reducing the sag problem with PE pipe resins. A high crystallization rate leads to fast hardening of the molten polymers and reduces the residual stresses caused by differing shrinkages in the surfaces versus core regions. For example, the crystallization rate of a HDPE/3wt% UHMWPE blend increased significantly as indicated by $T_{1/2}$ values decreasing from 13.4 min in the pure HDPE to 5.7 min in the blend. The higher crystallization rate achieved by the addition of UHMWPE led to a

DOI 10.1002/pen

reduction in pipe sag and faster pipe hardening. Similar benefits may be achieved in other types of industrial extrusion processes where sag or residual stresses occur [4, 75, 76].

HDPE film that was nucleated with a 0.2 wt% 1,3:2,4-bis(3,4-dimethylbenzylidene sorbitol NA was found to have enhanced clarity. The crystallization temperature increased from 109.1°C in the virgin HDPE resin to 109.8°C in the nucleated resin indicating its effectiveness as a NA. The resulting clarity values improved significantly from 70.4% in the virgin resin to 94.9% in the nucleated resin. Haze values dropped from 99.1% in the virgin resin to 88.7% in the nucleated resin. It is presumed that the smaller spherulites that result from the NA account for these optical changes [51].

The addition of NA can affect the flexural modulus of HDPE. HDPE containing three NAs, 0.05 wt% disodium bicycle [2.2.1]hepatane-2,3-dicarboxylate, 0.45 wt% impact PP copolymer, and 0.5 wt% $CaCO_3$, was injection molded into bars and the resulting flexural modulus was measured at differing storage times at room temperature after injection molding. The flexural modulus increased in the nucleated bars at all storage times. For example, after 10 h the flexural modulus went from 610 MPa in the virgin resin to 655 MPa in the nucleated sample. This increase in modulus could be a product of the resulting spherulites size or the degree of crystallization of these injection-molded parts. However, no explanation was provided to explain the reason for the increased modulus [66].

Likewise, extrusion blow molding studies were carried out in order to measure cycle time improvements in 350 ml HDPE bottle production. The minimum cycle time was recorded in each case, which was defined as the shortest cycle time that repeatedly yielded bottles without defects. Each tested sample involved reducing the cycle time by 0.5 s and then evaluating the quality of the produced bottle. These studies showed that the cycle time could be reduced by 25% or from about 12 to 9 s in a sample nucleated with 1000 ppm of the disodium bicyclo [2.2.1] heptane-2.3-dicarboxylate [66]. This enhancement is most likely a result of NA increasing the rate of crystallization.

In patent application US2012/0101209 halloysite nanotubular clay (HNT) is claimed to be an effective NA in HDPE at 0.1–1 wt% loading resulting in both reduced postextrusion shrinkage and improved clarity The preferred HNT has a median particle size of 0.01 to 20 μm (d50) and is melt mixed into the HDPE. Only a single cooling rate of 2.5°C/min was evaluated. The T_c was increased by about 1.9°C versus the neat HDPE, corresponding to an increased crystallization rate. The 1.9°C increase is considered quite significant and would be greater at higher cooling rates. The patent application states that this NA can provide a similar benefit in many types of polymer processes including extrusion, injection molding, spinning, and clear film production. In film extrusion the faster crystallization rate produces smaller and less developed spherulites, which improves film clarity. The increased rate of crystallization also yields reduced postextrusion shrinkage by reducing secondary crystallization processes that can cause further volume reduction and shrinkage in the solid state. A significant reduction in injection molding cycle time for samples with the HNT was observed, including a 24% reduction in mold cycle time with the HDPE sample containing 1 wt% HNT [59].

Over the last decade, Milliken & Company developed and commercialized an effective NA product called Hyperform™ HPN-20E for HDPE (calcium hexahydrophthalate) primarily to reduce cycle time and improve blow molding performance. HPN-20E is a high aspect ratio rod-shaped organic salt with an average particle width of 2.8 μm (see also NA Table 1). The unique shape of this NA enables its particles to align in the polymer flow direction especially in melt processes with nonturbulent laminar flow. HPN-20E has been used as a NA in a wide variety of polymer melt processes including extrusion, blown film, injection molding, and extrusion blow molding and is typically used in packaging applications [3].

As with all effective NAs, HPN-20E causes an increased peak T_c when present in HDPE. Milliken reported a T_c of 121.4°C with the HPN-20E/HDPE blend as compared to 118.5°C for the neat HDPE sample. Studies showed the increased T_c value enabled substantial reduction in cycle times (10–20%) in the injection molding of caps and closures [3].

Studies were also conducted on injection blow-molded bottles using HDPE nucleated with HPN-20E. The nucleated HDPE showed more consistent processing and improved dimensional stability as indicated by an improved neck ovality ratio enabling approximately 10% cycle time reduction [6, 7]. Likewise, a 15% improvement in water vapor and oxygen barrier properties is achieved in a substantially linear nucleated HDPE/HPN-20 film as compared to neat film of the same HDPE resin. The most dramatic improvement in barrier properties applies only to a specific linear HDPE resin with minimal long chain branching (LCB) and a narrow molecular weight distribution [67]. In one example, 0.1 wt% HPN-20E is melt blended into the linear HDPE and converted into a 1.25 mil thick film on a blown film line. A control film is also produced under the same processing conditions without the NA. The improvements in both water vapor and oxygen barrier were 46 and 50%. Similar improvements in these barrier properties were also achieved with zinc monoglycerolate (Irgastab™ 287) as NA. The combination of mica and HPN-20E in HDPE showed synergistic improvements in oxygen barrier properties. The improvements were better than the oxygen barrier values obtained with each of the components used alone. The patent application hypothesizes that the HPN-20 does not provide an improved physical barrier to oxygen but rather causes improved orientation of the crystalline lamellae which then leads to a more effective barrier to oxygen. The mica component may provide a physical barrier and increase the orientation of the crystalline lamellae for improved barrier properties [77].

This improved cycle time is expected in any type of extrusion process, including blown film extrusion. Dotson [78] reported a drop in frost line height in LLDPE in a blown film process which was attributed to the faster crystallization kinetics in a nucleated LLDPE sample with Hyperform HPN-20E. Similar improvements would be expected in HDPE blown film. The drop in frost line height can allow for increases in extruder throughput or line speed. Line speed increases of 5–20% were seen in one particular trial but these results would also depend on other factors such as machine configuration and process conditions [6, 7]. DSC studies showed that the crystallization temperature was increased by about 5° in LLDPE with HPN-20E as compared to the 3° in a HDPE/HPN-20E sample. Both increases are highly significant. Nucleated film thickness variation may also be improved due to more uniform crystallization of the polymer with NA [78].

A combination of NAs can reduce both the cycle time and coefficient of friction with a synergistic combination of 1 wt% talc as a NA and 0.1 wt% behanamide as slip agent melt mixed into bimodal HDPE. The preferred talc had a mean particle size (d50) of 1–10 μm. Increased T_c values were measured with the combination of talc and behanamide as compared to the T_c values with the talc or behenamide alone. The patent application example shows that the neat resin has a T_c of 117.5°C versus 118.4 and 118.8°C for the HDPE/1 wt% talc and HDPE/0.1 wt% behenamide samples, respectively. However, the combination of 1 wt% talc plus 0.1 wt% behenamide has a much higher T_c of 120.2°C. The coefficient of friction also improved with the HDPE/talc/behenamide sample as compared to the neat HDPE, and the samples with talc and behenamide alone [79].

Notably it has been shown that a NA can have a significant negative effect, particularly on the barrier properties. Utilizing a NA called Irgastab™ NA 11 [methylene-bis-(4,6-di-*tert*-butylphenyl) phosphate sodium salt] caused an 11% reduction in water vapor transmission and a 23% reduction in oxygen transmission versus the control sample. Also comparative examples of nonlinear HDPE and HPN-20E with LCB $>$ 0.5 and MFR $>$ 65, both of which are outside of the claimed ranges, showed relatively little improvement in both water and oxygen barrier properties. The reason for the specificity of this NA was not discussed.

Processing and Melt Flow Effects

In polymer processing, flow of material in the melt state can also play a major role in the crystallization of semicrystalline polymers such as HDPE. Therefore, the specific thermal and rheological conditions imparted onto the polymer during processing, which include shear stresses, elongational effects, and molecular orientation, can be used to control the final properties of the HDPE. Flow-induced crystallization is beyond the scope of this article and is only briefly mentioned here.

In the melt state HDPE polymer chains are easily deformed, elongating and orienting themselves in the direction of polymer flow. This polymer chain alignment and stretching affects the kinetics, thermodynamics, and final crystal morphology of HDPE. Generally, crystallization processes that occur during polymer flow show increased T_c, nucleation, and crystallization rates. The behavior of NAs during deformation is further complicated by particle–particle interactions mediated by hydrodynamics and viscoelasticity. Control of final properties of HDPE may be achieved by improved understanding of structure–property relationships that result from variations in processing type and conditions [80].

CONCLUSION AND FUTURE OUTLOOK

The crystallization process in HDPE was shown to significantly affect its optical, mechanical, and thermal properties. The amount of crystallization and the type of crystals formed are controlled by thermal history, cooling rate, and NA additives. Owing to widespread use of HDPE in many applications there is continued interest in gaining a deeper understanding of the crystallization process. Greater control over the crystallization process is needed in order to achieve further improvements in specific properties. However, it will first be necessary to overcome significant gaps in current understanding of the crystallization process and how to achieve better control over it by selecting or creating NAs.

To this end a deeper understanding of the affects of NA molecular structure and physical affects that occur during the crystallization process are needed. Although not yet at the level of control that is reached with NAs in PP, progress has been made in identifying effective NAs for HDPE and achieving a range of property improvements as was seen in many examples in this article.

Optimizing these properties leads to reduced spherulite sizes and an increased T_c. It is not yet known whether spherulite sizes can be further reduced or whether further increases in T_c can be achieved to approach levels of improvement similar to those reached with nucleated PP.

Gaps in understanding the optimum molecular structure for achieving optimal NA effectiveness in HDPE also need to be resolved. Only general principles are known about how molecular structure and characteristics impact NA efficiency as outlined in this article, including solubility/insolubility, polarity, and dispersion within HDPE. These characteristics relate to molecular structure in a more qualitative sense only. Discovering the optimum molecular characteristics for nucleating HDPE could lead to a custom-tailored NA molecule. An ultimate goal in this field would be to understand the crystallization process such that NAs could be engineered specifically to optimize NA melt dispersion, nucleation, crystallization, and final crystallization fraction using a cost-effective method.

REFERENCES

1. E. Ergoz, J.G. Fatou, and L. Mandelkern, *Macromolecules*, **5**, 147 (1972).
2. K.H. Buschow, R.W. Cahn, M.C. Flemings, B. Ilschner, E.J. Kramer, S. Mahajan, *Encyclopedia of Materials—Science and Technology, Volumes 1-11: Polyethylene: High-Density*, Elsevier, Amsterdam, 7178 (2001).
3. N. Farmer, *Trends in Packaging of Food Beverages and other Fast-Moving Consumer Goods (FMCG)—Markets Materials and Technologies*, Woodhead Publishing, Oxford, UK, 85 (2013).
4. S. Song, P. Wu, M. Ye, J. Feng, and Y. Yang, *Polymer*, **49**, 2964 (2008).
5. K. Nezhad, H. Orang and M. Motallebi, "The Effects of Adding Nano-Calcium Carbonate Particles on the Mechanical and Shrinkage Characteristics and Molding Process Consistency of PP/nano-$CaCO_3$ Nanocomposite," in *Polypropylene*, F. Dogan, Ed., InTech, Rijeka, Croatia (2012).
6. W. Van de Velde, "Newest Developments in the Nucleation of Polyethylene and Its Effects on Physical Properties Performance," in *SPE—International Polyolefins Conference*, Houston, March 1 (2011).
7. M. Tolinski, *Additives for Polyolefins: Getting the Most out of Polypropylene, Polyethylene, and TPO*, William Andrew, Oxford, UK, 166 (2009).
8. B. Wunderlich, *Thermal Analysis of Polymeric Materials*, Springer, Berlin, Heidelberg, 262 (2005).
9. A. Peacock and A. Calhoun, *Polymer Chemistry—Properties and Applications*, Hanser Publishers, Munich, 125 (2006).
10. M.L. Di Lorenzo and C. Silvestre, *Prog. Polym. Sci.*, **24**, 917 (1999).

 DOI 10.1002/pen

11. P.E. Malacari, *Effect of Both Talc Fineness and Talc Loading on Heterogeneous Nucleation of Block Copolymer Polypropylene*, SPE Antec, Orlando, FL, 2264 (2010).
12. J.P. Mercier, *Polym. Eng. Sci.*, **30**, 270 (1990).
13. M. Dong, K. Xu, H. Zou, and L.Y. Zhang, *"Excellent Properties of a Novel Composite β-Nucleating Agent for Isotactic Polypropylene," ANTEC® 2013—Proceedings of the Technical Conference & Exhibition*, Society of Plastics Engineers, Cincinnati, OH, 2180 (2013).
14. V. Cornelia and P. Mihaela, *Practical Guide to Polyethylene*, Smithers Rapra Technology, 94 (2005).
15. D. Kang, *Proceedings of the 58*th *International Wire and Cable Symposium*, 210 (2008).
16. K. Hoffman, G. Huber, and D. Mader, *Macomol. Symp.*, **176**, 83 (2001).
17. C. Maier and T. Calafut, *Polypropylene—The Definitive User's Guide & Databook*, William Andrew Publishing Plastics Design Library, CRC Press, Norwich, NY, 34 (1998).
18. A. Peacock, *Handbook of Polyethylene Structures, Properties and Applications*, CRC Press, NY, 101 (2000).
19. J.M. Fischer, *Handbook of molded Part Shrinkage and Warpage*, Elsevier, William Andrew Publishing Plastics Design Library, Norwich, NY, 26 (2013).
20. K.H. Bushow, *"Bulk Crystallization," in Encyclopedia of Materials—Science and Technology, Polymer Crystallization: General Concepts of Theory and Experiments*, Vol.1-11, Elsevier, Amsterdam, 7247 (2001).
21. L.H. Sperling, *Introduction to Physical Polymer Science*, 2nd ed., Wiley, New York, 232 (1992).
22. P. Zou, S. Tang, Z. Fu, and H. Xiong, *Int. J. Therm. Sci.*, **48**, 837 (2009).
23. M. Muthukumar, "Nucleation in Polymer Crystallization," in *Advances in Chemical Physics*, S.A. Rice, Ed., John Wiley & Sons, Hoboken, NJ, **128**, 1 (2004).
24. M.E. Brown and P.K. Gallagher, *Handbook of Thermal Analysis and Calorimetry—Recent Advances, Techniques and Applications, Volume 5: 13.4.1 Crystallization*, Elsevier, Amsterdam, 514 (2008).
25. M. Joshi and B.S. Butola, *J. Appl. Polym. Sci.*, **105**, 978 (2007).
26. X. Chen, J. Shi, L. Wang, H. Shi, Y. Liu, and L. Wang, *Polym. Compos.*, **32**, 177 (2010).
27. T. Kanai and G. Campbell, *Film Process*, Hanser Publishers, Vol. 167 (1999).
28. M. Avrami, *J. Chem. Phys.*, **7**, 1103 (1939).
29. M. Avrami, *J. Chem. Phys.*, **8**, 212 (1940).
30. M. Avrami, *J. Chem. Phys.*, **9**, 177 (1941).
31. A.T. Lorenzo, M.L. Arnal, J. Albuerne, and A. Muller, *Polym. Test.*, **26**, 222 (2007).
32. G. Liang, J. Xu, and W. Xu, *J. Appl. Polym. Sci.*, **91**, 3054 (2004).
33. S. Wang and J. Zhang, *Therm. Anal. Calorim.*, **115**, 63 (2014).
34. Q. Jiasheng and H. Pingsheng, *J. Mater. Sci.*, **38**, 2299 (2003).
35. D. Grenier and R.E.P. Homme, *J. Poly. Sci. Part B*, **18**, 1655 (1980).
36. C. Silvestre and S. Cimmino, *Crystallization, Morphology and Melting in Polymer Blends*, Smithers Rapra Technology, New York, 439 (2002).
37. K. Nakamura, K. Katayama, and T. Amano, *J. Appl. Polym. Sci.*, **17**, 1031 (1973).
38. J.A. Martins and J.J.C. Pinto, *Polymer*, **41**, 6875 (2000).
39. A. Jeziorny, *Polymer*, **19**, 1142 (1978).
40. I.A. Hussein, *J. Appl. Polym. Sci.*, **107**, 2802 (2008).
41. M. Eder and A. Wlochowicz, *Polymer*, **24**, 1593 (1983).
42. T. Liu, Z. Mo, S. Wang, and H. Zhang, *Polym. Eng. Sci.*, **37**, 568 (1997).
43. J.W. Huang, Y.L. Wen, C.C. Kang, W.J. Tseng, and M. Yeh, *Polym. Eng. Sci.*, **48**, 1268 (2008).
44. G.M. Benedikt, *Metallocene Technology in Commercial Applications—34.4.3 Activation Energy for Non-Isothermal Melt Crystallization by Kissinger Method*, William Andrew Publishing/Plastics Design Library, Norwich, NY (1999).
45. L.A. Utracki, *Clay-Containing Polymeric Nanocomposites, Volumes 1-2: 3.4.2 Fundamentals of Crystallisation*, Smithers Rapra Technology, NY, 396 (2004).
46. F.L. Binsbergen, *Polymer*, **11**, 253 (1970).
47. H. Kissinger, *J. Res. Natl. Bureau Stand.*, **57**, 217 (1956).
48. B. Risch, *ANTEC, Plastics: Plastics on My Mind, Vol. 1: Processing "Influence of Nucleating Agent and Melt Flow Index on the Impact Polypropylene Fiber Optic Buffer Tubes*, Society of Plastics Engineers, Atlanta, GA, 1016 (1998).
49. F.C. Chiu and Q. Fu, *ANTEC, 3*, Society of Plastics Engineers, New York (1999).
50. Y.P. Khanna, *Macromolecules*, **26**, 3639 (1993).
51. S. Sahebian, S.M. Zebarjad, J.V. Khaki, and S.A. Sajjadi, *J. Mater. Process. Technol.*, **209**, 1310 (2009).
52. W. Zheng, X. Lu, and S.C. Wong, *J. Appl. Polym. Sci.*, **91**, 2781 (2004).
53. W. Zheng, S.C. Wong, and H.J. Sue, *Polymer*, **43**, 6767 (2002).
54. M. Joshi and B.S. Butola, *Polymer*, **45**, 4953 (2004).
55. J.F. Vega, J.M. Salazar, M. Trujillo, M.L. Arnal, A.J. Miller, S. Bredeau, and Ph. Dubois, *Macromolecules*, **42**, 4719 (2009).
56. M. Trujillo, M.L. Arnal, A.J. Muller, E. Laredo, and S.T. Bredeau, *Macromolecules*, **40**, 6268 (2007).
57. M. Trujillo, M.L. Arnal, and A.J. Muller, *Macromolecules*, **41**, 2087 (2008).
58. S.C. Tjong and S.P. Tjong, *J. Polym. Sci. Part B: Polym. Phys.*, **43**, 253 (2005).
59. Y.P. Khanna, A. Dharia, and A.M. Zeitoun, U.S. Patent 0,101,209 (2012).
60. A. Choudhury, *Mater. Sci. Eng.*, **491**, 492 (2008).
61. H. Ishida and P. Bussi, *Macromolecules*, **24**, 3569 (1991).
62. M. Horrocks, C. Kerscher, and D. Dotson, *A Novel Nucleating Agent for Polyethylene*, The Plastics And Rubber Institute of Singapore, Tanglin, Singapore, **29** (2008).
63. L.M. Sherman, "Polyolefin Additives: Pushing the Limits in Films & Molded Parts," in *Plastics Technology*, Plastics Technology, Cincinnati, OH (2014).
64. J.C. Wittmann and B. Lotz, *J. Polym. Sci.: Polym. Phys. Ed.*, **19**, 1837 (1981).
65. P. Wijga, U.S. Patent 3,207,735 (Shell Oil Company) (1960).
66. R. Hanssen, M.B. Barker, N.A. Mehl, W.S. Wolters, S.M. Bernhardt, and A.T. Radwanski, U.S. Patent 7786203B2 (Milliken and Company) (2010).

67. J.S. Borke, D.C. McFaddin, and S.M. Imfeld, U.S. Patent 0,225,742 (Equistar Chemicals) (2013).
68. H.N. Beck and H.D. Ledbetter, *J. Appl. Polym. Sci.*, **9**, 2131 (1965).
69. H.N. Beck, *J. Appl. Polym. Sci.*, **11**, 673 (1967).
70. L. Minkova and M. Mihailov, *Colloid Polym. Sci.*, **267**, 577 (1989).
71. L. Minkova and M. Mihailov, *Colloid Polym. Sci.*, **265**, 1 (1987).
72. L. He, Q. Xu, R. Song, and C. Hua, *Polym. Compos.*, **31**, 913 (2010).
73. M. Gahleitner, C. Grein, S. Kheirandish, and J. Wolfschwenger, *Intern. Polym. Process., XXVI*, 1 (2011).
74. A. Lazzeri, S.M. Zebarjad, M. Pracella, K. Cavalier, and R. Rosa, *Polymer*, **46**, 827 (2005).
75. P.J. Deslauriers, M.P. McDaniel, D.C. Rohlfing, R.K. Krishnswamy, S.J. Secora, E.A. Benham, P.L. Maeger, A.R. Wolfe, A.M. Sukhadia, and B.B. Beaulieu, *Polym. Eng. Sci.*, **45**, 1203 (2005).
76. E. Zopf, A. Arellano, S. Tyagi, A, Tynys, J. Braun, and M. Gahleitner, WO2013060736 (Borealis AG) (2013).
77. J.R. De Oliveira, A, Rangel, B. Mano, C. DeLemos, and F. Decarvhalho, WO2014/091309 (Braskem S.A.) (2014).
78. D.L. Dotson, *"A Novel Nucleating Agent for Polyethylene," in 2007 Proceedings of the 2007 PLACE conference*, St. Louis, MO (2011).
79. K. Bhawna, M. Luc, and B. Laurent, WO2012/000958 (2012).
80. B. Vergnes, M. Vincent, and J. Haudin, *Design of Extrusion Forming Tools*, Smithers Rapra Technology, Shawbury, UK, **55** (2012).
81. A. Ziabicki, *Appl. Polym. Symp.*, **6**, 1 (1967).

 DOI 10.1002/pen